Elsevier Editorial System(tm) for Free Radical Biology and Medicine
Manuscript Draft

Manuscript Number: FRBM-D-11-00397R2

Title: Induction of glutathione synthesis and heme oxygenase 1 by the flavonoids butein and phloretin is mediated through the ERK/Nrf2 pathway and protects against oxidative stress

Article Type: Original Contribution

Keywords: Butein; CCl4; ERK; Glutamate cysteine ligase; Heme oxygenase 1; Nrf2; Phloretin; tBHP

Corresponding Author: Dr. Haw-Wen Chen,

Corresponding Author's Institution: China Medical University

First Author: Ya-Chen Yang

Order of Authors: Ya-Chen Yang; Chong-Kuei Lii; Ai-Hsuan Lin; Yu-Wen Yeh; Hsien-Tsung Yao; Chien-Chun Li; Kai-Li Liu; Haw-Wen Chen

Abstract: Butein and phloretin are chalcones that are members of the flavonoid family of polyphenols. Flavonoids have well-known antioxidant and anti-inflammatory activities. In rat primary hepatocytes, we examined whether butein and phloretin affect tert-butyl hydroperoxide (tBHP)-induced oxidative damage and the possible mechanism(s) involved. Treatment with butein and phloretin markedly attenuated tBHP-induced peroxide formation, and this amelioration was reversed by l-buthionine-S-sulfoximine [a glutamate cysteine ligase (GCL) inhibitor] and zinc protoporphyrin [a heme oxygenase 1 (HO-1) inhibitor]. Butein and phloretin induced both HO-1 and GCL protein and mRNA expression and increased intracellular glutathione (GSH) and total GSH content. Butein treatment activated the ERK1/2 signaling pathway and increased Nrf2 nuclear translocation, Nrf2 nuclear protein-DNA binding activity, and ARE-luciferase reporter activity. The role of the ERK signaling pathway and Nrf2 in butein-induced HO-1 and GCL catalytic subunit (GCLC) expression was determined by using RNA interference directed against ERK2 and Nrf2. Both siERK2 and siNrf2 abolished butein-induced HO-1 and GCLC protein expression. These results suggest the involvement of ERK2 and Nrf2 in the induction of HO-1 and GCLC by butein. In animal study, phloretin was shown to increase GSH content and HO-1 expression in rat liver and decrease carbon tetrachloride (CCl4)-induced hepatotoxicity. In conclusion, we demonstrated that butein and phloretin up-regulate HO-1 and GCL expression through the ERK2/Nrf2 pathway and protect hepatocytes against oxidative stress.

Free Radical Biology and Medicine

Dr. Kevin Peter Moore

Manuscript No.: FRBM-D-11-00397R1

Dear Dr. Moore:

Upon the requirement of FRBM, we have uploaded a separate document with article highlights.

Thank you.

Sincerely,

Haw-Wen Chen, Ph.D.
Department of Nutrition
China Medical University
Tel: 886-4-22053366 Ext. 7520
Fax: 886-4-22062891
Email: chenhw@mail.cmu.edu.tw

Highlights

Butein and phloretin induce HO-1 and GCL expression. Enhanced GCL expression leads to increased hepatic GSH synthesis. ERK2/Nrf2 pathway plays a key role in the induction of HO-1 and GCL by butein. Induction of HO-1 and GCL protects liver against oxidative stress.

*Revised Manuscript (text UNmarked)
Click here to view linked References

Induction of glutathione synthesis and heme oxygenase 1 by the flavonoids butein and phloretin is mediated through the ERK/Nrf2 pathway and protects against oxidative stress

Ya-Chen Yang [a,1], Chong-Kuei Lii [b,1], Ai-Hsuan Lin [c], Yu-Wen Yeh [b], Hsien-Tsung Yao [b], Chien-Chun Li [c], Kai-Li Liu [c], Haw-Wen Chen [b,*]

[a] Department of Health and Nutrition Biotechnology, Asia University, Taichung, Taiwan

[b] Department of Nutrition, China Medical University, Taichung, Taiwan

[c] Department of Nutrition, Chung Shan Medical University, Taichung, Taiwan

[*] Corresponding author. Department of Nutrition, China Medical University, Taichung 404, Taiwan. Fax: +886 4 2206 2891.

E-mail address: chenhw@mail.cmu.edu.tw (H.-W. Chen).

[1] These authors contributed equally to this work.

ABSTRACT

Butein and phloretin are chalcones that are members of the flavonoid family of polyphenols. Flavonoids have well-known antioxidant and anti-inflammatory activities. In rat primary hepatocytes, we examined whether butein and phloretin affect *tert*-butyl hydroperoxide (tBHP)-induced oxidative damage and the possible mechanism(s) involved. Treatment with butein and phloretin markedly attenuated tBHP-induced peroxide formation, and this amelioration was reversed by l-buthionine-S-sulfoximine [a glutamate cysteine ligase (GCL) inhibitor] and zinc protoporphyrin [a heme oxygenase 1 (HO-1) inhibitor]. Butein and phloretin induced both HO-1 and GCL protein and mRNA expression and increased intracellular glutathione (GSH) and total GSH content. Butein treatment activated the ERK1/2 signaling pathway and increased Nrf2 nuclear translocation, Nrf2 nuclear protein-DNA binding activity, and ARE-luciferase reporter activity. The role of the ERK signaling pathway and Nrf2 in butein-induced HO-1 and GCL catalytic subunit (GCLC) expression was determined by using RNA interference directed against ERK2 and Nrf2. Both siERK2 and siNrf2 abolished butein-induced HO-1 and GCLC protein expression. These results suggest the involvement of ERK2 and Nrf2 in the induction of HO-1 and GCLC by butein. In animal study, phloretin was shown to increase GSH content and HO-1 expression in rat liver and decrease carbon

tetrachloride (CCl_4)-induced hepatotoxicity. In conclusion, we demonstrated that butein and phloretin up-regulate HO-1 and GCL expression through the ERK2/Nrf2 pathway and protect hepatocytes against oxidative stress.

Keywords: Butein; CCl_4; ERK; Glutamate cysteine ligase; Heme oxygenase 1; Nrf2; Phloretin; tBHP

Introduction

The excessive production of reactive oxygen species (ROS) is associated with cell damage and the development of chronic diseases in humans [1]. Therefore, compounds with antioxidant properties may be useful for preventing oxidative stress-mediated diseases [2]. Cardiovascular disease (CVD) is a common chronic disease and is the leading cause of morbidity and mortality in the United States [3]. Atherosclerosis is one of the major causes of CVD, and it is well established that oxidative stress and inflammation play a critical role in atherosclerosis [4]. From the evidence, it is inferred that compounds with antioxidant and anti-inflammatory properties may exert protective effects against CVD. In support of this, a large cohort study demonstrated an inverse correlation between total fruit and vegetable intake and risk of CVD [5].

Flavonoids are naturally occurring polyphenolic compounds and represent one of the most prevalent classes in fruits, vegetables, nuts, and beverages such as tea, coffee, and red wine [6] as well as in medical herbs [7]. Flavonoids are composed of flavones, flavonols, flavanones, flavanols, chalcones, anthocyanins, and isoflavones. Flavonoids are well known for their capacity as antioxidant and anti-inflammatory agents and are reported to have health-promoting, disease-preventing, and chemopreventive activities [8].

Glutathione (GSH) is an endogenously synthesized tripeptide thiol that is involved in numerous basic cellular processes including maintaining redox status [9], scavenging free radicals and electrophilic intermediates [10], conjugation/detoxification reactions [11], apoptosis [12], and cell signaling [13]. Glutamate cysteine ligase (GCL) catalyzes the rate-limiting step in GSH synthesis; it is a heterodimeric protein composed of catalytic (GCLC) and modifier (GCLM) subunits that are expressed by distinct genes [14]. Both *in vivo* and *in vitro* models in broccoli seeds have shown that the induction of GCLC expression is dependent on nuclear factor erythroid 2-related 2 (Nrf2) [15]. Nrf2 is a transcription factor that is necessary for the induction of numerous phase II enzymes [16]. Under basal conditions, Nrf2 is retained in the cytosol by binding to Klech-like ECH-associated protein 1 (Keap1) [17]. The Keap1-Nrf2 complex is disrupted in response to several electrophilic antioxidants, and free Nrf2 translocates to the nucleus, where it binds to the antioxidant/electrophile response element (ARE) sequences of the target gene promoter, in conjunction with small Maf proteins [18]. AREs are found in the promoters of many antioxidant and detoxifying enzyme genes, including GCLC, GSH *S*-transferase (GST), and heme oxygenase 1 (HO-1) [19]. HO-1 is an inducible enzyme and catalyzes the rate-limiting step of free heme degradation into Fe^{2+}, carbon monoxide, and biliverdin, the last of which is subsequently catabolized into bilirubin

by biliverdin reductase [20]. HO-1 is known for its cytoprotective effects against oxidative stress [21] and plays an important role in the resolution of inflammation [22].

Butein and phloretin are chalcones that are members of the flavonoid family and that have well-known antioxidant and anti-inflammatory activities. Although these antioxidant and anti-inflammatory properties of the chalcones are well known, however, few studies have investigated the potential of the chalcones to activate cellular antioxidant and anti-inflammatory genes such as HO-1 and GCL and the specific transcription factor and upstream signaling kinases involved in HO-1 and GCL expression. In this study, therefore, we investigated the role of Nrf2 and upstream signaling kinases involved in the induction of HO-1 and GCL expression by butein and phloretin in rat primary hepatocytes. Furthermore, we investigated the role of HO-1 and GCL in protection against *tert*-butyl hydroperoxide (tBHP)- and CCl_4-induced oxidative damage.

Materials and methods

Chemicals

Cell culture medium (RPMI-1640) and penicillin-streptomycin solution were obtained from Gibco Laboratory (Grand Island, NY). TRIzol was purchased from Invitrogen (Carlsbad, CA). Zinc protoporphyrin (ZnPP) was purchased from Calbiochem (La Jolla, CA). Dexamethasone, 3-(4,5-dimethylthiazol-2-yl)-2,5-diphenyltetrazolium bromide (MTT), HEPES, l-buthionine-S-sulfoximine (BSO), butein, and phloretin were obtained from Sigma Chemical (St. Louis, MO). ITS^+ (insulin, transferrin, selenium, bovine serum albumin, and linoleic acid) was obtained from BD Biosciences (San Jose, CA). Small interfering RNAs (siRNAs) against Nrf2 and ERK2 were purchased from Dharmacon (Lafayette, CO). Glutamic oxaloacetic transaminase (GOT) and glutamic pyruvic transaminase (GPT) kits were obtained from Randox Laboratories Ltd, (UK).

Hepatocyte isolation and culture

Male Sprague-Dawley rats at 5 to 6 weeks of age were obtained from the

BioLASCO Experimental Animal Center (Taipei, Taiwan). Hepatocytes were isolated by a modification of the two-step collagenase perfusion method described previously [23]. After isolation, hepatocytes ($3x10^6$ cells/dish) were plated on collagen-coated 60-mm plastic tissue dishes (Falcon, Franklin Lakes, NJ) in RPMI-1640 medium (pH 7.37) supplemented with 10 mM Hepes, 1% ITS^+, 1 μM dexamethasone, 100 IU penicillin/ml, and 100 μg streptomycin/ml. Cells were incubated at 37°C in a 5% CO_2 humidified incubator. After 4 h, the cells were washed with phosphate-buffered saline to remove any unattached or dead cells, and the same medium supplemented with 0.1 μM dexamethasone was added. Twenty hours after attachment, cells were treated with various concentrations of butein or phloretin. The protocol for each experiment is described in the corresponding figure legend.

Cell viability assay

Cell viability was analyzed by MTT assay. The MTT assay measures the ability of viable cells to reduce a yellow 3-(4,5-dimethylthiazol-2-yl)-2,5-diphenyltetrazolium bromide to a purple formazan by mitochondrial succinate dehydrogenase. After incubation with 10, 25, and 50 μM butein or phloretin for 24 h, or 25 μM butein or phloretin for 24 h followed by challenge with 0.5 mM tBHP for an

additional 12 h, the medium was removed, and hepatocytes were then incubated in RPMI-1640 medium containing 0.5 mg/ml MTT for an additional 3 h. The medium was then removed, and isopropanol was added to dissolve the formazan. After centrifugation at 7,000×*g* for 5 min, the supernatant of each sample was transferred to 96-well plates, and absorbance was read at 595 nm in an ELISA reader. The absorbance in cultures treated with 0.1% DMSO was regarded as 100% cell viability.

RNA isolation and RT-PCR

Total RNA of hepatocytes was extracted by using TRIzol reagent. After treatment, cells were washed twice with cold PBS and scraped with 500 μl of TRIzol reagent. Cell samples were mixed with 100 μl of chloroform and centrifuged at 11,000×*g* for 15 min. The supernatant was collected and mixed with 250 μl of isopropyl alcohol. After centrifugation at 12,000×*g* for 20 min, the supernatant was discarded and the RNA precipitate was stored in 70% ethanol or dissolved in deionized water for quantification. We used 0.2 μg of total RNA for the synthesis of first-strand cDNA by using Moloney murine leukemia virus reverse transcriptase (Promega Company, Madison, WI) in a 20-μl final volume containing 250 ng oligo(dT) and 40 U RNase inhibitor. PCR was carried out in a thermocycler in a 50-μl

reaction volume containing 20 μl of cDNA, BioTaq PCR buffer, 50 μM of each deoxyribonucleotide triphosphate, 1.25 mM $MgCl_2$, and 1 U of BioTaq DNA polymerase (GENET BIO, Chungnam, Korea). Oligonucleotide primers of HO-1 (forward: 5'-AGCATGTCCCAGGATTTGTC-3'; reverse: 5'-AAGGCGGTCTTAGCCTCTTC-3'), GCLC (forward: 5'-CCTTCTGGCACAGCACGTTG-3'; reverse: 5'-TAAGACGGCATCTCGCTCCT-3'), and glyceraldehyde 3-phosphate dehydrogenase (GAPDH) (forward: 5'-CCATCACCATCTTCCAGGAG-3'; reverse: 5'-CCTGCTTCACCACCTTCTTG-3') were designed on the basis of published sequences [24,25]. Amplification of HO-1 and GAPDH was performed by heating samples to 95°C for 5 min and then immediately cycling 25 times through a 30-s denaturing step at 94°C, a 45-s annealing step at 56°C, and a 45-s elongation step at 72°C. For GCLC amplification, the PCR cycle number was 32 times through a 60-s denaturing step at 94°C, a 60-s annealing step at 60°C, and a 90-s elongation step at 72°C. The GAPDH cDNA level was used as the internal standard. PCR products were resolved in a 1%-agarose gel and were scanned by using a Digital Image Analyzer (Alpha Innotech) and quantitated with ImageGauge software (FUJIFILM Science Lab).

Measurement of intracellular reduced and oxidized GSH content

After treatment with butein or phloretin for 24 h, 100 μl of the cytosolic fraction of hepatocytes was reacted with 200 μl of 10 mM Ellman's reagent by gentle mixing, and followed by adding 60 μl of 20% 5-sulfosalicylic acid to cause acid precipitation. After centrifugation at 10,000x*g* and 4^{o}C for 10 min, 100 μl of supernatant was used to analyze reduced and oxidized GSH content by use of a High-Performance Liquid Chromatography-Mass Spectrophotometer (HPLC/MS, Hewlett Packard) [26].

Plasmids, transfection, and luciferase assays

A p2xARE/Luc fragment containing tandem repeats of double-stranded oligonucleotides spanning the Nrf2 binding site, 5'-TGACTCAGCA-3', was introduced into the pGL3 promoter plasmid (Promega). All subsequent transfection experiments were performed by using nanofection reagent (PAA, Pasching, Austria) according to the manufacturer's instructions. For luciferase assays, the cell lysate was first mixed with a luciferase substrate solution (Promega), and the resulting luciferase activity was measured by using a microplate luminometer (TROPIX TR-717, Applied Biosystems). For each experiment, luciferase activity was determined in triplicate and

was normalized with β-galactosidase activity.

RNA interference by small interfering RNA

Hepatocytes were transfected with ERK2 or Nrf2 siRNA SMARTpool by using DharmaFECT1 transfection reagent (Thermo, Rockford, IL) according to the manufacturer's instructions. The 4 siRNAs against the rat ERK2 gene are (1) ACACUAAUCUCUCGUACAU, (2) AAAAUAAGGUGCCGUGGAA, (3) UAUACCAAGUCCAUUGAUA, and (4) UCGAGUUGCUAUCAAGAAA. The 4 siRNAs against the rat Nrf2 gene are (1) GAACACAGAUUUCGGUGAU, (2) AGACAAACAUUCAAGCCGA, (3) GGGUUCAGUGACUCGGAAA, and (4) AGAAUAAAGUUGCCGCUCA. A nontargeting control-pool siRNA was also tested and was used as the negative control. After 24 h of transfection, cells were treated with butein or phloretin for another 24 h. Cell samples were collected for Western blotting analysis.

Nuclear extract preparation

After each experiment, cells were washed twice with cold PBS and were then

scraped from the dishes with 1000 μl of PBS. Cell homogenates were centrifuged at 2,000×*g* for 5 min. The supernatant was discarded, and the cell pellet was allowed to swell on ice for 15 min after the addition of 200 μl of hypotonic buffer containing 10 mM HEPES, 1 mM $MgCl_2$, 1 mM EDTA, 10 mM KCl, 0.5 mM DTT, 0.5% Nonidet P-40, 4 μg/ml leupeptin, 20 μg/ml aprotinin, and 0.2 mM PMSF. After centrifugation at 6,000×*g* for 15 min, pellets containing crude nuclei were resuspended in 50 μl of hypertonic buffer containing 10 mM HEPES, 400 mM KCl, 1 mM $MgCl_2$, 0.25 mM EDTA, 0.5 mM DTT, 4 μg/ml leupeptin, 20 μg/ml aprotinin, 0.2 mM PMSF, and 10% glycerol at 4^{o}C for 30 min. The samples were then centrifuged at 10,000×*g* for 15 min. The supernatant containing the nuclear proteins was collected and stored at -80^{o}C until the Western blotting and electrophoretic mobility shift assays.

Western blotting analysis

Cells were washed twice with cold PBS and were harvested in 150 μl of lysis buffer (10 mM Tris-HCl, pH 8.0, 0.1% Triton X-100, 320 mM sucrose, 5 mM EDTA, 1 mM PMSF, 1 μg/ml leupeptin, 1 μg/ml aprotinin, and 2 mM dithiothreitol). Cell homogenates were centrifuged at 10,000×*g* for 20 min at 4^{o}C. The resulting supernatant was used as a cellular protein for Western blotting analysis. The

preparation of nuclear extracts was described above. The total protein was analyzed by use of the Coomassie Plus protein assay reagent kit (Pierce Biotechnology Inc., Rockford, IL). Equal amounts of proteins were electrophoresed in an SDS-polyacrylamide gel, and proteins were then transferred to polyvinylidene fluoride membranes. Nonspecific binding sites on the membranes were blocked with 5% nonfat milk in 15 mM Tris/150 mM NaCl buffer (pH 7.4) at room temperature for 2 h. Membranes were probed with anti-GCLC (Abcam, Cambridge, UK), anti-Nrf2 (Santa Cruz), anti-HO-1 (Calbiochem, San Diego, CA), anti-ERK, anti-phospho-ERK, anti-JNK, anti-phospho-JNK, anti-p38, anti-phospho-p38, anti-Akt, anti-phospho-Akt, anti-PARP (Cell Signaling Technology), anti-GAPDH (Millipore, Billerica, MA), and anti-actin (Sigma) antibodies. The membranes were then probed with the secondary antibody labeled with horseradish peroxidase. The bands were visualized by using an enhanced chemiluminescence kit (PerkinElmer Life Science, Boston, MA) and were scanned by a luminescent image analyzer (FUJIFILM LAS-4000, Japan). The bands were quantitated with ImageGauge software.

Electrophoretic mobility shift assay

Electrophoretic mobility shift assay (EMSA) was performed according to our

previous study [27]. The LightShift Chemiluminescent EMSA Kit (Pierce Chemical Company, Rockford, IL) and synthetic biotin-labeled double-stranded rHO-1 ARE consensus oligonucleotides (forward: 5′-AACCATGACACAGCATAAAA-3′; reverse: 5′-TTTTATGCTGTGTCATGGTT-3′) were used to measure Nrf2 nuclear protein-DNA binding activity. Five micrograms of nuclear extract, poly (dI-dC), and biotin-labeled double-stranded ARE oligonucleotides were mixed with the binding buffer (Chemiluminescent Nucleic Acid Detection Module, Thermo, Rockford, IL) to a final volume of 20 μl, and the mixture was incubated at room temperature for 30 min. Unlabeled double-stranded rHO-1 ARE oligonucleotides and mutant double-stranded oligonucleotides (5′- AACCAgtcCACAGCATAAAA -3′) were used to confirm the protein-binding specificity. The nuclear protein-DNA complex was separated by electrophoresis on a 6% TBE-polyacrylamide gel and was then transferred to a Hybond-N^+ nylon membrane. The membranes were cross-linked by UV light for 10 min and were then reacted with 20 μl of streptavidin-horseradish peroxidase for 20 min, and the nuclear protein-DNA bands were developed with a Chemiluminescent Substrate (Thermo). The bands were scanned by a luminescent image analyzer (FUJIFILM LAS-4000, Japan).

Peroxide measurement

Detection of intracellular oxidative states was performed by using the probe 2,7-dichlorofluorescin diacetate (H_2DCF-DA; Molecular Probes Inc., Eugene, OR). Hepatocytes were pretreated with butein or phloretin for 24 h before being challenged with 0.5 mM tBHP for 1 h. To assess the effects of the inhibitors BSO (a GCL inhibitor) and ZnPP (a HO-1 inhibitor), cells were pretreated with the respective inhibitor for 2 h before the addition of butein or phloretin. As a control, an equal amount of DMSO was added to untreated cells. After treatment, cells were incubated with 5 μmol/l of H_2DCF-DA for 10 min. The DCF fluorescence was then detected by a Confocal Microscope Detection System (Leica TCS SP2).

Animal study

Male Sprague-Dawley rats (weighing 200-220 g) received i.p. injection of 10 or 30 mg/kg phloretin for 5 consecutive days. At day 6, animals were sacrificed and liver tissues were removed for HO-1 expression and GSH content determination as described above. For the carbon tetrachloride (CCl_4) experiment, rats were i.p. administrated with 30 mg/kg phloretin for 5 consecutive days and then 1 ml/kg CCl_4 (50% in olive oil) was i.p. injected at day 6. Animals were sacrificed after 24 h and blood was withdrawn for GOT and GPT activity assay according to the

manufacturer's instructions. The rats were treated in compliance with the Guide for the Care and Use of Laboratory Animals [28].

Statistical analysis

Data were analyzed by using analysis of variance (SAS Institute, Cary, NC). The significance of the difference among mean values was determined by one-way analysis of variance followed by the Tukey's test and the difference between mean values was determined by Student's t-test. *P* values <0.05 were taken to be statistically significant.

Results

Concentration changes in butein and phloretin during cell culture

To determine the concentration changes in butein and phloretin during cell culture, the remaining percentage of butein and phloretin in the media was determined by HPLC/MS during 24 h of treatment (Fig. 1). In the cell-free condition, concentrations of butein (A) and phloretin (B) gradually decreased and 80% and 55% were left, respectively, after 4 h. With hepatocytes, contents of chalcones dropped quickly and the remaining percentages of both butein (A) and phloretin (B) at 4 h were only 15% and 10%, respectively. The decreased remaining percentage in presence of hepatocytes may implicate the uptake or degradation of butein and phloretin by hepatocytes.

Effects of butein and phloretin on cell viability

We used the MTT assay to test whether the concentrations of butein and phloretin used in the present study caused cell damage. The cell viabilities of rat primary hepatocytes treated with 10, 25 or 50 μM butein and phloretin were

108.0±5.1%, 100.2±5.2%, 96.1±7.9%, 100.2±6.7%, 93.3±0.6%, and 92.9±5.0%, respectively, compared with the unstimulated controls (100%). As indicated, there were no adverse effects on the growth of rat primary hepatocytes up to a concentration of 50 μM butein or phloretin. Thereafter, the highest concentration of butein and phloretin used in this study was 25 μM.

Butein and phloretin alleviate tBHP-induced oxidative damage through the induction of HO-1 and GCLC

Oxidative stress plays a key role in the pathogenesis of several chronic diseases. Oxidative stress can be induced *in vitro* by use of numerous oxidants, including hydrogen peroxide, tBHP, 4-hydroxynonenal, sodium arsenite, and UV irradiation [29]. In the present study, we used tBHP to induce oxidative damage and to investigate the protective effects of butein and phloretin. As shown in Fig. 2A, cell viability was significantly decreased in cells treated with 0.5 mM tBHP for 12 h. In cells pretreated with 25 μM butein or phloretin, damage was significantly attenuated ($p < 0.05$). Cellular peroxide formation was also measured in cells, as shown in Fig. 2B, peroxide formation was significantly greater in cells treated with 0.5 mM tBHP for 1 h than in control cells. Cells pretreated with 25 μM butein or phloretin for 24 h

and then challenged with 0.5 mM tBHP for an additional 1 h showed significantly less peroxide formation than did cells treated with tBHP alone (pictures c and d vs. b). In cells pretreated with BSO or ZnPP for 2 h, the protective effect of butein on peroxide formation was abolished (pictures e and f). Thus, the induction of GCLC and HO-1 at least partially explains the antioxidant activity of butein and phloretin.

*Butein and phloretin increase GSH, total GSH, GSH/oxidized GSH (GSH/GSSG), and GCLC expression in hepatocy*tes

Compared to control hepatocytes, hepatocytes treated with 5, 10, or 25 μM butein and phloretin for 24 h had significantly greater cellular GSH, total GSH, and GSH/GSSG (p<0.05) (Table 1). It is reported that GCL catalyzes the rate-limiting step in GSH synthesis [14]. Because of the increased cellular GSH content with butein and phloretin treatments, we determined the effects of butein and phloretin on GCLC protein expression. As shown in Fig. 3A, treatment with both butein and phloretin for 24 h induced GCLC protein expression in a dose-dependent manner. These results suggest that the enhanced GCLC protein expression contributes to the increased cellular GSH content. In addition to protein expression, GCLC mRNA expression was affected by butein and phloretin treatments. Treatment with both 10 and 25 μM butein

and phloretin significantly induced GCLC mRNA expression (p<0.05) (Fig. 3B).

Butein and phloretin induce HO-1 expression in hepatocytes

HO-1 is an inducible enzyme that catalyzes the rate-limiting step in the degradation of free heme. Because of the well-known antioxidant and anti-inflammatory activities of HO-1, compounds with HO-1-inducing activity are recognized to have cytoprotective properties. Butein (5, 10, and 25 μM) and phloretin (25 μM) significantly induced HO-1 protein expression (p<0.05) (Fig. 3C).We also observed the induction of HO-1 mRNA expression by butein and phloretin (Fig. 3D).

ERK and Nrf2 activation in butein and phloretin induction of HO-1 and GCLC expression

Nrf2 activation can be under the regulation of protein kinase C, phosphatidylinositol 3-kinase (PI3K)/Akt, and mitogen-activated protein kinase [30]. The effect of chalcones on kinase signaling pathway was performed with butein but not with phloretin. To clarify the importance of the kinase signaling pathway in the induction of HO-1 and GCLC by butein, we treated rat primary hepatocytes with 25

μM butein for 0.5, 1, 2, 3, 6, and 12 h. As shown in Fig. 4A, ERK1/2 phosphorylation occurred 0.5 h after treatment ($p<0.05$), and phosphorylation declined at 6 h after treatment. However, no effect of butein on the activation of the other mitogen-activated protein kinases and Akt was observed (data not shown). The role of ERK2 in butein-induced HO-1 and GCLC protein expression was further investigated. As shown in Fig. 4B, silencing ERK2 attenuated the butein-induced HO-1 and GCLC protein expression. In addition, silencing ERK2 abolished the butein-induced nuclear accumulation of Nrf2 (Fig. 4C). These data imply that ERK1/2 may be the candidate kinase for Nrf2 activation and nuclear translocation and subsequent HO-1 and GCLC induction by butein.

Nrf2 is a transcription factor necessary for the induction of numerous antioxidant and detoxification phase II enzymes [16], and it binds to the ARE sequences of target gene promoters in conjunction with small Maf proteins. Nrf2 undergoes nuclear translocation and induces gene expression in response to stress. As shown in Fig. 5A, cells treated with 25 μM butein had a higher level of Nrf2 accumulation in the nuclear fraction as early as 1 h, and this accumulation was sustained until 12 h. However, the level of cytosolic Nrf2 was relatively stable throughout the 12 h of treatment with 25 μM butein (Fig. 5A). Our results are consistent with the finding reported by Kim et al. [31] that phytochemical-induced HO-1 expression is mediated by Nrf2.

Furthermore, we used EMSA to determine the effects of butein and phloretin on Nrf2 nuclear protein-DNA binding activity. As shown in Fig. 5B, 25 μM butein and phloretin increased the DNA binding activity of Nrf2. We further used cells transfected with luciferase reporter constructs harboring the ARE to determine the specificity of butein and phloretin for this sequence. As shown in Fig. 5C, both 25 μM butein and phloretin significantly increased ARE-luciferase activity ($p<0.05$).

Next, we examined the role of Nrf2 in the induction of HO-1 and GCLC protein expression by butein by using an siRNA SMARTpool system to create an Nrf2-knockdown model. Hepatocytes were transfected with an siNrf2 construct for 24 h, followed by treatment with 25 μM butein for an additional 24 h. Control cells were transfected with a nontargeting siRNA construct. The efficiency of the siRNA SMARTpool system in knocking down Nrf2 was assayed by Western blot (Fig. 6). Knockdown of Nrf2 expression, the induction of HO-1 and GCLC protein expression by butein was apparently abolished (Fig. 6).

Phloretin increases rat liver GSH content and HO-1 expression and decreases CCl_4-induced hepatotoxicity

Male Sprague-Dawley rats receiving i.p. injection of 10 and 30 mg/kg phloretin

for 5 consecutive days had significantly greater GSH content in liver. The GSH contents of rats treated with 0, 10 or 30 mg/kg phloretin were 5.0±0.8, 7.3±0.7, and 7.2±1.2 μmol/g liver (n=4). We also found that the induction of liver HO-1 expression by phloretin treatment (Fig. 7). Next, we determined whether phloretin treatment decreases CCl_4-induced hepatotoxicity. As shown in Table 2, rats receiving 30 mg/kg phloretin for 5 consecutive days followed by i.p. injection of CCl_4 (1 ml/kg, 50% in olive oil) had significantly less plasma GOT and GPT activities. Thus, the inhibition of CCl_4-induced hepatotoxicity by phloretin might be attributed to its increased hepatic GSH content and HO-1 expression.

Discussion

In this study, we demonstrated that both butein and phloretin effectively suppressed tBHP-induced oxidative damage and that this inhibition was likely associated with an up-regulation of HO-1 and GCLC expression through the ERK2/Nrf2 pathway. We also found that rats receiving phloretin treatment had significantly less CCl_4-induced hepatotoxicity.

Oxidative stress is a state wherein the balance between the free radicals generated and the free radical or oxidant scavenging capacity of the endogenous antioxidant system is disrupted. Oxidative stress is documented to be involved in the pathogenesis of several chronic diseases [1]. Cellular antioxidants are composed of oxidant scavengers and antioxidant enzymes that convert free radicals to more benign molecules. Thiol-containing compounds such as GSH and thioredoxin are oxidized by free radicals and rapidly regenerated. GSH is an endogenously synthesized tripeptide thiol, and GCL catalyzes the rate limiting step in GSH synthesis [14].

HO-1 is an inducible enzyme that catalyzes the rate-limiting step of free heme degradation into Fe^{2+}, carbon monoxide, and biliverdin, the last of which is subsequently catabolized into bilirubin by biliverdin reductase [20]. Accumulating evidence indicates that induction of HO-1 expression protects against various chronic

diseases, including atherosclerosis, diabetes, obesity, cardiovascular disease, and hypertension [21,32]. In a previous review, Ryter et al. [33] described that increased HO-1 expression is associated with increased antioxidant protection. The antioxidant function of bilirubin has been demonstrated both *in vivo* and *in vitro*. For example, the addition of bilirubin in micromolar concentrations in cell culture media protects against cytotoxicity induced by H_2O_2 in bovine vascular smooth muscle cells [34]. In addition, increased HO-1 expression and bilirubin accumulation are involved in heme-conferred resistance to H_2O_2-mediated cytotoxicity in vascular smooth muscle cells. The antioxidant activity of bilirubin was demonstrated *in vivo* in the jaundiced Gunn rat model [35]. Jaundiced Gunn rats with hyperbilirubinemia display a reduced manifestation of plasma biomarkers of oxidative stress in response to hyperoxia compared with their nonjaundiced counterparts.

Hyperglycemia has been linked to oxidative stress and leads to endothelial cell dysfunction. Streptozotocin-induced diabetic rats have significantly greater levels of circulating endothelial cells and urinary output of 8-epi-isoprostane PGF2α, an indicator of overall oxidative stress, than do their normal counterparts [36]. Diabetic rats receiving daily i.p. injection of CORM-3, a CO donor, exhibit a greater than 6-fold increase in plasma CO levels compared with that in rats receiving vehicle. CO significantly decreases circulating endothelial cells and urinary output of

8-epi-isoprostane PGF2α in diabetic animals ($p<0.05$).

It is reported that acute administration of iron to intact rats [37] or to rat hepatoma cells [38] induces the synthesis of the iron-storage protein ferritin. The cytoprotective antioxidant role of ferritin has been demonstrated in porcine aorta endothelial cells [39]. There is an inverse correlation between endothelial cell ferritin and H_2O_2/hemin-mediated cytotoxicity.

Enhancement of intracellular antioxidant capacity is believed to reduce the risk of oxidative stress-mediated diseases. Chalcones are one kind of flavonoids that are recognized to have health-promoting, disease-preventing, and chemopreventive activities because of their antioxidant and anti-inflammatory properties. Compared with the other flavonoids, however, few studies have investigated the antioxidant potential of chalcones including butein and phloretin. In the present study, we found that butein and phloretin significantly suppressed tBHP-induced peroxide formation (Fig. 2B), and that this inhibition was attenuated by BSO (a GCL inhibitor) and ZnPP (a HO-1 inhibitor). Our results imply that the antioxidant activity of butein and phloretin is associated with their induction of GCLC and HO-1. Butein and phloretin were shown to induce GCLC and HO-1 protein and mRNA expression *in hepatocytes* (Figs. 3A, 3B, 3C, and 3D), and phloretin was shown to induce HO-1 protein expression in rat liver (Fig. 7). Consistent with the GCLC protein and mRNA results,

cells treated with butein and phloretin had significantly greater cellular GSH, total GSH, and GSH/GSSG than did control cells (Table 1), and the GSH-enhancing effect of phloretin in rat liver was demonstrated as well.

It is well established that Nrf2 activation is under the regulation of protein kinase C, phosphatidylinositol 3-kinase (PI3K)/Akt, and mitogen-activated protein kinase [30]. Sulforaphane induces Nrf2 activity, induces GCL activity, and increases cellular GSH content, and these actions are mediated by the PI3K/Akt pathway [40]. Nrf2 is reported to be phosphorylated at Ser-40 by protein kinase C, and this phosphorylation leads to Nrf2 dissociation from Keap1 [41]. Subsequently, free Nrf2 transactivates ARE-mediated transcription. It has been demonstrated that activation of p38 MAPK and an increase in the nuclear level of Nrf2 are involved in gallic acid-induced P-form phenol sulfotransferase expression in human hepatoma HepG2 cells [42]. In addition, Nrf2 has also been shown to play a critical role in the ARE-driven gene expression of HO-1 [43]. Supporting this idea, we examined the effect of butein on the protein expression of Nrf2 as well as the nuclear accumulation of Nrf2. In the present study, butein was found to activate ERK (Fig. 4A), and to increase the nuclear accumulation of Nrf2 (Fig. 5A), increase Nrf2 nuclear protein-DNA binding activity (Fig. 5B), and increase ARE-luciferase reporter activity (Fig. 5C). To further determine the signaling pathway and transcription factor involved in butein-induced HO-1 and GCLC

expression, we used RNA interference directed against ERK2 and Nrf2. Both siERK2 and siNrf2 abolished butein-induced HO-1 and GCLC protein expression (Figs. 4B and 6).

Our results suggest the involvement of ERK2 and Nrf2 in the induction of HO-1 and GCLC by butein. The findings of this study are schematically presented in Fig. 8. In conclusion, we have shown that butein and phloretin inhibit tBHP-induced oxidative damage by up-regulating HO-1 and GCLC expression through the ERK2/Nrf2 pathway and that phloretin suppresses CCl_4-induced hepatotoxicity via the enhancement of hepatic GSH content and HO-1 expression. The antioxidant property of butein and phloretin confers them with protective activity against oxidative stress-mediated diseases.

Acknowledgements

This work was supported by grant CMU99-ASIA-09.

Abbreviations

ARE, antioxidant/electrophile response element; BSO, l-buthionine-S-sulfoximine; CCl_4, carbon tetrachloride; CVD, cardiovascular disease; EMSA, electrophoretic mobility shift assay; GAPDH, glyceraldehyde 3-phosphate dehydrogenase; GCL, glutamate cysteine ligase; GCLC, glutamate cysteine ligase catalytic subunit; GCLM, glutamate cysteine ligase modifier subunit; GOT, glutamic oxaloacetic transaminase; GPT, glutamic pyruvic transaminase; GSH, glutathione; GST, glutathione S-transferase; HO-1, heme oxygenase 1; ITS^+, insulin, transferrin, selenium, bovine serum albumin, and linoleic acid; Keap1, Klech-like ECH-associated protein 1; MTT, 3-(4,5-dimethylthiazol-2-yl)-2,5-diphenyltetrazolium bromide; Nrf2, nuclear factor erythroid 2-related 2; ROS, reactive oxygen species; siRNA, small interfering RNA; tBHP, *tert*-butyl hydroperoxide; ZnPP, zinc protoporphyrin.

References

[1] Cooke, M. S.; Evans, M. D.; Dizdaroglu, M.; Lunec, J. Oxidative DNA damage: mechanisms, mutation, and disease. *FASEB J.* **17**:1195-1214; 2003.

[2] Mayne, S. T. Antioxidant nutrients and chronic disease: use of biomarkers of exposure and oxidative stress status in epidemiologic research. *J. Nutr.* **133(3 Suppl)**:933S-940S; 2003.

[3] Anderson, R. N. Deaths: leading causes for 1999. In: National vital statistics reports. Vol 49. Atlanta (GA): Centers for Disease Control and Prevention; 2001.

[4] Singh, U.; Devaraj, S.; Jialal, I. Vitamin E, oxidative stress, and inflammation. *Annu. Rev. Nutr.* **25**:151-174; 2005.

[5] Hung, H. C.; Joshipura, K. J.; Jiang, R.; Hu, F. B.; Hunter, D.; Smith-Warner, S. A.; Colditz, G. A.; Rosner, B.; Spiegelman, D.; Willett, W. C. Fruit and vegetable intake and risk of major chronic disease. *J. Natl. Cancer Inst.* **96**:1577-1584; 2004.

[6] Hollman, P. C.; Katan, M. B. Absorption, metabolism and health effects of dietary flavonoids in man. *Biomed. Pharmacother.* **51**:305-310; 1997.

[7] Moon, Y. J.; Wang, X.; Morris, M. E. Dietary flavonoids: effects on xenobiotic and carcinogen metabolism. *Toxicol. In Vitro* **20**:187-210; 2006.

[8] Nijveldt, R. J.; van Nood, E.; van Hoorn, D. E.; Boelens, P. G.; van Norren, K.; van Leeuwen, P. A. Flavonoids: a review of probable mechanisms of action and potential applications. *Am. J. Clin. Nutr.* **74**:418-425; 2001.

[9] Jones, D. P. Redox potential of GSH/GSSG couple: assay and biological significance. *Methods Enzymol.* **348**: 93-112; 2002.

[10] Kidd, P. M. Glutathione: systemic protectant against oxidative and free radical damage. *Altern. Med. Rev.* **2**:155-176; 1997.

[11] Chan, K.; Han, X. D.; Kan, Y. W. An important function of Nrf2 in combating oxidative stress: detoxification of acetaminophen. *Proc. Natl. Acad. Sci. USA* **98**:4611-4616; 2001.

[12] Honda, T.; Coppola, S.; Ghibelli, L.; Cho, S. H.; Kagawa, S.; Spurgers, K. B.; Brisbay, S. M.; Roth, J. A.; Meyn, R. E.; Fang, B.; McDonnell, T. J. GSH depletion enhances adenoviral bax-induced apoptosis in lung cancer cells. *Cancer Gene Ther.* **11**:249-255; 2004.

[13] Reddy, N. M.; Kleeberger, S. R.; Cho, H. Y.; Yamamoto, M.; Kensler, T. W.; Biswal, S.; Reddy, S. P. Deficiency in Nrf2-GSH signaling impairs type II cell

growth and enhances sensitivity to oxidants. *Am. J. Respir. Cell Mol. Biol.* **37**:3-8; 2007.

[14] Franklin, C. C.; Backos, D. S.; Mohar, I.; White, C. C.; Forman, H. J.; Kavanagh, T. J. Structure, function, and post-translational regulation of the catalytic and modifier subunits of glutamate cysteine ligase. *Mol. Aspects Med.* **30**:86-98; 2009.

[15] McWalter, G. K.; Higgins, L. G.; McLellan, L. I.; Henderson, C. J.; Song, L.; Thornalley, P. J.; Itoh, K.; Yamamoto, M.; Hayes, J. D. Transcription factor Nrf2 is essential for induction of NAD(P)H:quinone oxidoreductase 1, glutathione S-transferases, and glutamate cysteine ligase by broccoli seeds and isothiocyanates. *J. Nutr.* **134(12 Suppl)**:3499S-3506S; 2004.

[16] Itoh, K.; Chiba, T.; Takahashi, S.; Ishii, T.; Igarashi, K.; Katoh, Y.; Oyake, T.; Hayashi, N.; Satoh, K.; Hatayama, I.; Yamamoto, M.; Nabeshima, Y. An Nrf2/small Maf heterodimer mediates the induction of phase II detoxifying enzyme genes through antioxidant response elements. *Biochem. Biophys. Res. Commun.* **236**:313-322; 1997.

[17] Itoh, K.; Tong, K. I.; Yamamoto, M. Molecular mechanism activating Nrf-2-keap1 pathway in regulation of adaptive response to electrophiles. *Free*

Radic. Biol. Med. **36**:1208-1213; 2004.

[18] Kong, A. N.; Owuor, E.; Yu, R.; Hebbar, V.; Chen, C.; Hu, R.; Mandlekar, S. Induction of xenobiotic enzymes by the MAP kinase pathway and the antioxidant or electrophile response element (ARE/EpRE). *Drug Metab. Rev.* **33**:255-271; 2001.

[19] Mulcahy, R. T.; Wartman, M. A.; Bailey, H. H.; Gipp, J. J. Constitutive and beta-naphthoflavone-induced expression of the human gamma-glutamylcysteine synthetase heavy subunit gene is regulated by a distal antioxidant response element/TRE sequence. *J. Biol. Chem.* **272**:7445-7454; 1997.

[20] Ryter, S. W.; Tyrrell, R. M. The heme synthesis and degradation pathways: Role in oxidant sensitivity: Heme oxygenase has both pro- and antioxidant properties. *Free Radic. Biol. Med.* **28**:289-309; 2000.

[21] Abraham, N. G.; Kappas, A. Heme oxygenase and the cardiovascularrenal system. *Free Radic. Biol. Med.* **39**:1-25; 2005.

[22] Pae, H. O.; Lee, Y. C.; Chung, H. T. Heme oxygenase-1 and carbon monoxide: emerging therapeutic targets in inflammation and allergy. *Recent Pat. Inflamm. Allergy Drug Discov.* **2**:159-165; 2008.

[23] Seglen, P. O. Preparation of isolated rat liver cells. *Methods Cell Biol.* **13**:29-83;

1976.

[24] Koriyama, Y.; Chiba, K.; Yamazaki, M.; Suzuki, H.; Muramoto, K.; Kato, S. Long-acting genipin derivative protects retinal ganglion cells from oxidative stress models in vitro and in vivo through the Nrf2/antioxidant response element signaling pathway. *J. Neurochem.* **115**:79-91; 2010.

[25] Yan, N.; Meister, A. Amino acid sequence of rat kidney gamma-glutamylcysteine synthetase. *J. Biol. Chem.* **265**:1588-1593; 1990.

[26] Yao, H. T.; Lin, P.; Chang, Y. W.; Chen, C. T.; Chiang, M. T.; Chang, L.; Kuo, Y. C.; Tsai, H. T.; Yeh, T. K. Effect of taurine supplementation on cytochrome P450 2E1 and oxidative stress in the liver and kidneys of rats with streptozotocin-induced diabetes. *Food Chem. Toxicol.* **47**:1703-1709; 2009.

[27] Cheng, W. L.; Lii, C. K.; Chen, H. W.; Lin, T. H.; Liu, K. L. Contribution of conjugated linoleic acid to the suppression of inflammatory responses through the regulation of the NF-kappaB pathway. *J. Agric. Food Chem.* **52**:71-78; 2004.

[28] National Research Council. Guide for the care and use of laboratory animals. Publication no. 85-23 (rev.). Bethesda (Md)7 National Institutes of Health; 1985.

[29] Allen, R. G.; Tresini, M. Oxidative stress and gene regulation. *Free Radic. Biol. Med.* **28**:463-499; 2000.

[30] Kensler, T. W.; Wakabayashi, N.; Biswal, S. Cell survival responses to environmental stresses via the Keap1-Nrf2-ARE pathway. *Annu. Rev. Pharmacol. Toxicol*. **47**:89-116; 2007.

[31] Kim, K. M.; Jung, D. H.; Jang, D. S.; Kim, Y. S.; Kim, J. M.; Kim, H. N.; Surh, Y. J.; Kim, J. S. Puerarin suppresses AGEs-induced inflammation in mouse mesangial cells: a possible pathway through the induction of heme oxygenase-1 expression. *Toxicol. Appl. Pharmacol.* **244**:106-113; 2010.

[32] Abraham, N. G.; Kappas, A. Pharmacological and clinical aspects of heme oxygenase. *Pharmacol. Rev.* **60**:79-127; 2008.

[33] Ryter, S. W.; Alam, J.; Choi, A. M. Heme oxygenase-1/carbon monoxide: from basic science to therapeutic applications. *Physiol. Rev.* **86**:583-650; 2006.

[34] Clark, J. E.; Foresti, R.; Green, C. J.; Motterlini, R. Dynamics of haem oxygenase-1 expression and bilirubin production in cellular protection against oxidative stress. *Biochem. J.* **348**:615-619; 2000.

[35] Dennery, P. A.; McDonagh, A. F.; Spitz, D. R.; Rodgers, P. A.; Stevenson, D. K. Hyperbilirubinemia results in reduced oxidative injury in neonatal Gunn rats

exposed to hyperoxia. *Free Radic. Biol. Med.* **19**:395-404; 1995.

[36] Rodella, L.; Lamon, B. D.; Rezzani, R.; Sangras, B.; Goodman, A. I.; Falck, J. R.; Abraham, N. G. Carbon monoxide and biliverdin prevent endothelial cell sloughing in rats with type I diabetes. *Free Radic. Biol. Med.* **40**:2198-2205; 2006.

[37] Aziz, N.; Munro, H. N. Both subunits of rat liver ferritin are regulated at a translational level by iron induction. *Nucleic Acids Res.* **14**:915-927; 1986.

[38] Rogers, J.; Munro, H. Translation of ferritin light and heavy subunit mRNAs is regulated by intracellular chelatable iron levels in rat hepatoma cells. *Proc. Natl. Acad. Sci. USA* **84**:2277-2281; 1987.

[39] Balla, G.; Jacob, H. S.; Balla, J.; Rosenberg, M.; Nath, K.; Apple, F.; Eaton, J. W.; Vercellotti, G. M. Ferritin: a cytoprotective antioxidant strategem of endothelium. *J. Biol. Chem.* **267**:18148-18153; 1992.

[40] Wang, L.; Chen, Y.; Sternberg, P.; Cai, J. Essential roles of the PI3 kinase/Akt pathway in regulating Nrf2-dependent antioxidant functions in the RPE. *Invest. Ophthalmol. Vis. Sci.* **49**:1671-1678; 2008.

[41] Huang, H. C.; Nguyen, T.; Pickett, C. B. Phosphorylation of Nrf2 at Ser-40 by protein kinase C regulates antioxidant response element-mediated transcription. *J. Biol. Chem.* **277**:42769-42774; 2002.

[42] Yeh, C. T.; Yen, G. C. Involvement of p38 MAPK and Nrf2 in phenolic acid-induced P-form phenol sulfotransferase expression in human hepatoma HepG2 cells. *Carcinogenesis* **27**:1008-10017; 2006.

[43] Prawan, A.; Keum, Y. S.; Khor, T. O.; Yu, S.; Nair, S.; Li, W.; Hu, L.; Kong, A. N. Structural influence of isothiocyanates on the antioxidant response element (ARE)-mediated heme oxygenase-1 (HO-1) expression. *Pharm. Res.* **25**:836-844; 2008.

Figure legends

Fig. 1. Concentration changes in butein and phloretin during cell culture. Butein and phloretin (25 μM) were added to the cell culture medium in absence of hepatocytes (⬥) or in presence of hepatocytes (■). Changes in butein (A) and phloretin (B) concentrations in the medium over 24 h were determined by HPLC-MS. Values are means ± SD of three independent experiments.

Fig. 2. Effects of butein and phloretin on tBHP-induced cell damage and peroxide formation. Cells were pretreated with 25 μM butein or phloretin for 24 h followed by challenge with 0.5 mM tBHP for an additional 12h (A). Cells were pretreated with butein and phloretin for 24 h before being challenged with tBHP for an additional 1 h. BSO and ZnPP were added 2 h before butein treatment. Cells treated with DMSO were used as the control (a). tBHP induced peroxide formation (b). Both butein (c) and phloretin (d) suppressed tBHP-induced peroxide formation. ZnPP (a HO-1 activity inhibitor) (e) and BSO (a GCL activity inhibitor) (f) reversed the inhibition of tBHP-induced peroxide formation by butein.

Fig. 3. Butein and phloretin induce GCLC and HO-1 protein and mRNA expression in rat primary hepatocytes. Cells were treated with 0-25 μM butein or phloretin for 24 h. Aliquots of total protein were used for GCLC (20 μg) (A) and HO-1 (10 μg) (C)

protein expression. Total RNA was isolated from cells and was subjected to RT-PCR with specific GCLC (B), HO-1 (D), and GAPDH primers as described in Materials and Methods. Values are means ± SD of three independent experiments. Values not sharing the same letter are significantly different ($p < 0.05$). One representative immunoblot from three independent experiments is shown.

Fig. 4. Effect of butein on ERK activation in rat primary hepatocytes, and the role of ERK2 in butein-induced HO-1 and GCLC expression. After attachment, hepatocytes were treated with 25 μM butein for various time periods and ERK phosphorylation was determined (A). After attachment, hepatocytes were transiently transfected with non-targeting control siRNA or siERK2 for 24 h, followed by treatment with 25 μM butein for an additional 24 h. siERK2 attenuated the butein-induced HO-1 and GCLC protein expression (B). Aliquots of nuclear protein (20 μg) were used for Western blot analysis. siERK2 abolished butein-induced Nrf2 nuclear accumulation (C).

Fig. 5. Effect of butein on Nrf2 activation. Cells were prepared after treatment with 25 μM butein for the indicated time periods. Immunoblots of nuclear, cytosolic, and total extracts from treated cells were then probed with the Nrf2-specific antibody (A). Nuclear extracts of cells treated with 10 and 25 μM butein or phloretin for 6 h were

used for Nrf2 nuclear protein DNA-binding activity (B). Aliquots of nuclear extracts (5 μg) were used for EMSA. To confirm the specificity of the nucleotide, 200-fold cold probe (biotin-unlabeled ARE binding site) and biotin-unlabeled double-stranded mutant ARE oligonucleotide (2 ng) were included in the EMSA. One representative experiment out of three independent experiments is shown. Cells were transfected with the ARE-luciferase construct for 12 h and were then stimulated with 25 μM butein and phloretin for an additional 24 h (C). The cells were then lysed and analyzed for luciferase activity. Values not sharing the same letter are significantly different ($p < 0.05$).

Fig. 6. Effect of siNrf2 on butein-induced HO-1 and GCLC expression in rat primary hepatocytes. After attachment, hepatocytes were transiently transfected with non-targeting control siRNA or siNrf2 for 24 h, followed by treatment with 25 μM butein for an additional 24 h. Nrf2 siRNA inhibited butein-induced HO-1 and GCLC expression.

Fig. 7. Effect of phloretin treatment on HO-1 expression in rat liver. Male Sprague-Dawley rats received i.p. injection of 30 mg/kg phloretin in 100 μl DMSO and PBS (50:50) (n=4) for 5 consecutive days. At day 6, animals were sacrificed and

HO-1 protein expression in pooled liver samples was determined.

Fig. 8. Scheme summarizing the inhibition of tBHP-induced oxidative damage by butein and phloretin via the up-regulation of HO-1 and GCLC expression through the ERK2/Nrf2 pathway and the suppression of CCl_4-induced hepatotoxicity by phloretin via the enhancement of hepatic GSH content.

Table 1

Effects of butein and phloretin on cellular GSH content[*].

Treatment	Dose (μM)	GSH (nmol/mg protein)	Total GSH (nmol/mg protein)	GSH/GSSG
Control		115.2±21.8[a]	116.7±22.1[a]	156.6±22.1[a]
butein	5	154.5±18.1[ab]	157.1±16.0[ab]	254.7±59.0[b]
	10	171.1±15.2[b]	172.3±15.3[b]	276.5±16.3[b]
	25	199.0±25.1[b]	200.5±25.4[b]	303.6±33.8[b]
phloretin	5	188.8±38.9[ab]	190.4±38.9[ab]	281.0±22.8[b]
	10	200.5±19.5[b]	201.9±19.4[b]	369.4±19.8[b]
	25	210.2±28.7[b]	211.6±28.6[b]	361.9±71.5[b]

[*] Values are means ± SD, n = 3. Twenty hours after attachment, hepatocytes were incubated with various concentrations of butein and phloretin for 24 h. Values not sharing a same letter are significantly different ($p < 0.05$).

Table 2

Effect of phloretin on carbon tetrachloride-induced hepatotoxicity*.

	CCl_4 treatment	control	phloretin
GOT (U/L)	before	24.1±5.9	25.1±9.4
	after	252±71.6	165.0±50.6 *
GPT (U/L)	before	22.0±4.9	15.2±4.8 *
	after	231.3±87.8	107.5±56.3 *

Values are means ± SD, n =7-8. Male Sprague-Dawley rats received i.p. injection of 30 mg/kg phloretin for 5 consecutive days followed by i.p. injection of 1 ml/kg carbon tetrachloride (CCl_4) (50% in olive oil). Rats were sacrificed after 24 h, and plasma was collected before and after 24 h CCl_4 treatment for GOT and GPT determinations.

*Means significant difference between control and phloretin groups ($p < 0.05$).

Figure(s)
Click here to download high resolution image

Fig. 1.

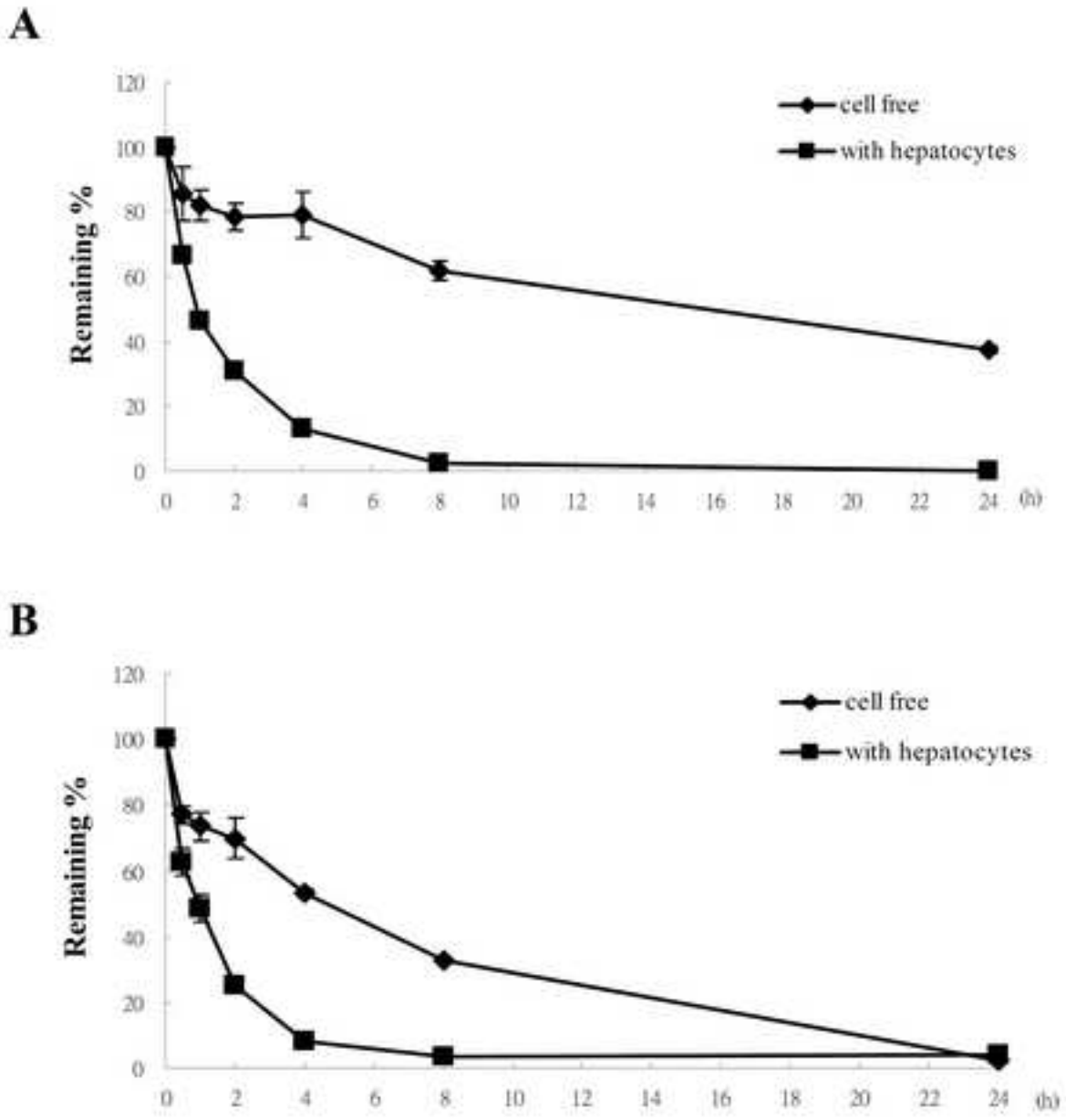

Figure(s)
Click here to download high resolution image

Fig. 2.

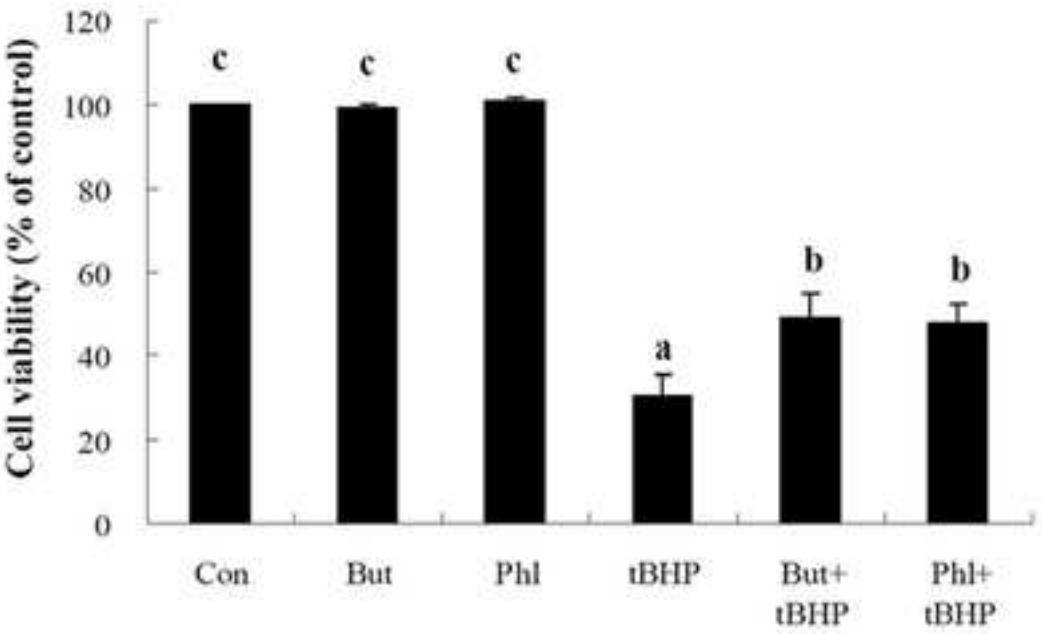

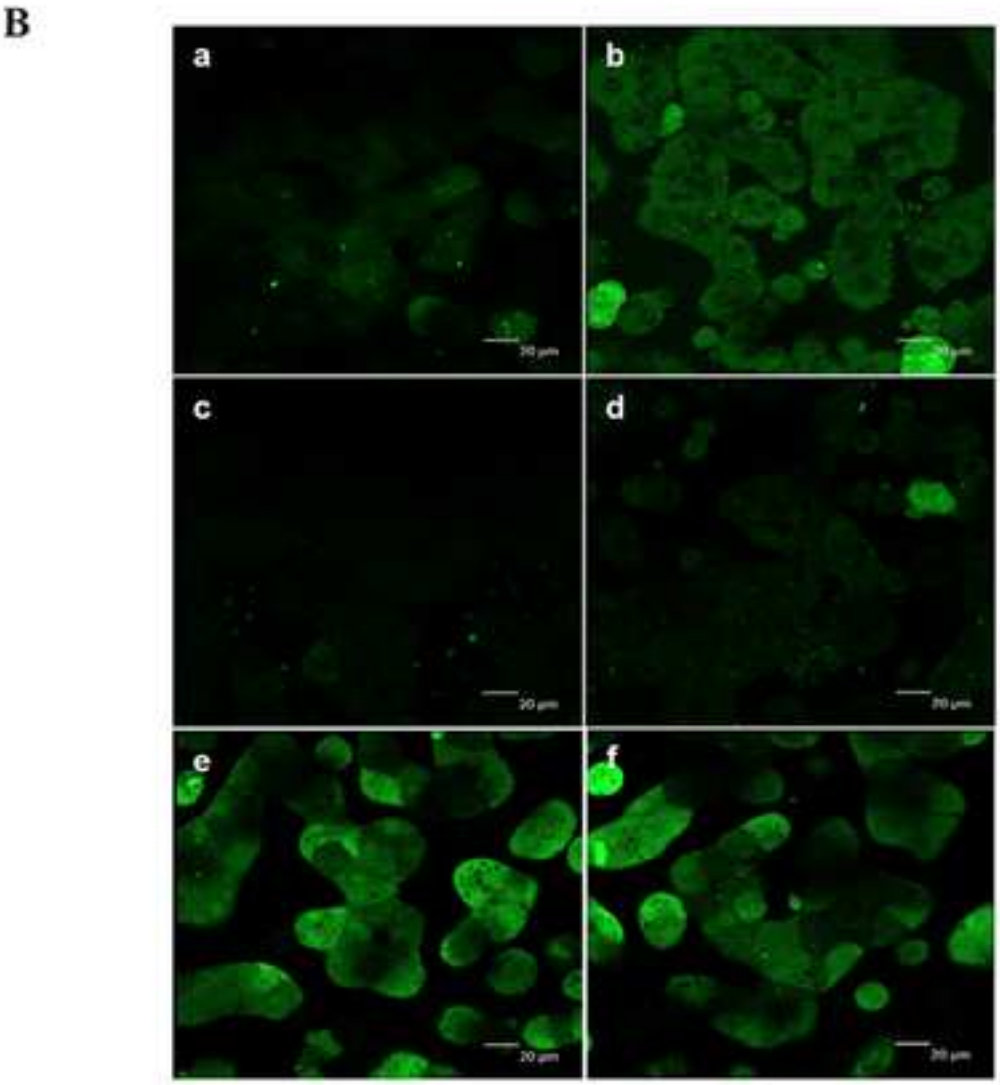

Figure(s)
Click here to download high resolution image

Fig. 3.

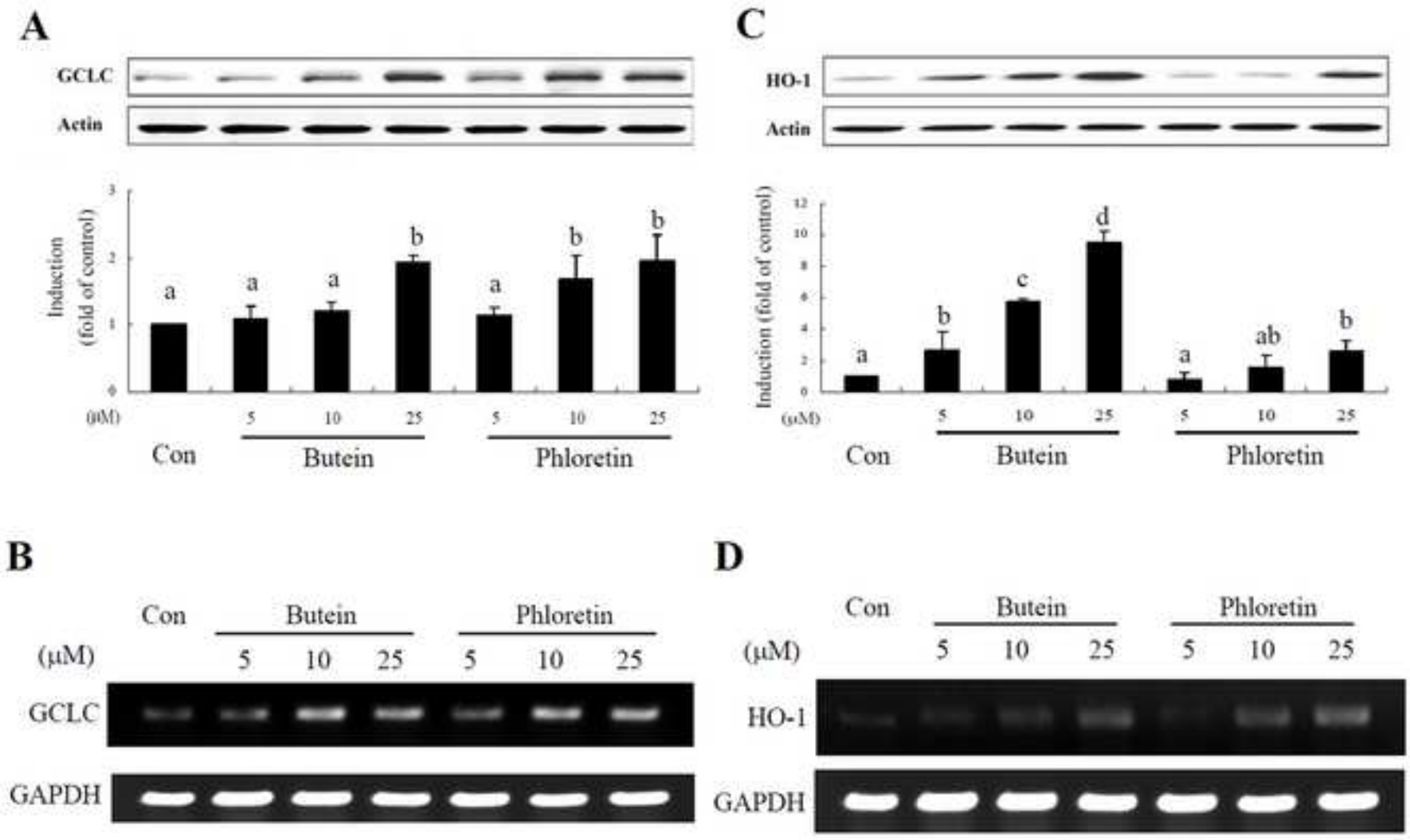

Figure(s)
Click here to download high resolution image

Fig. 4.

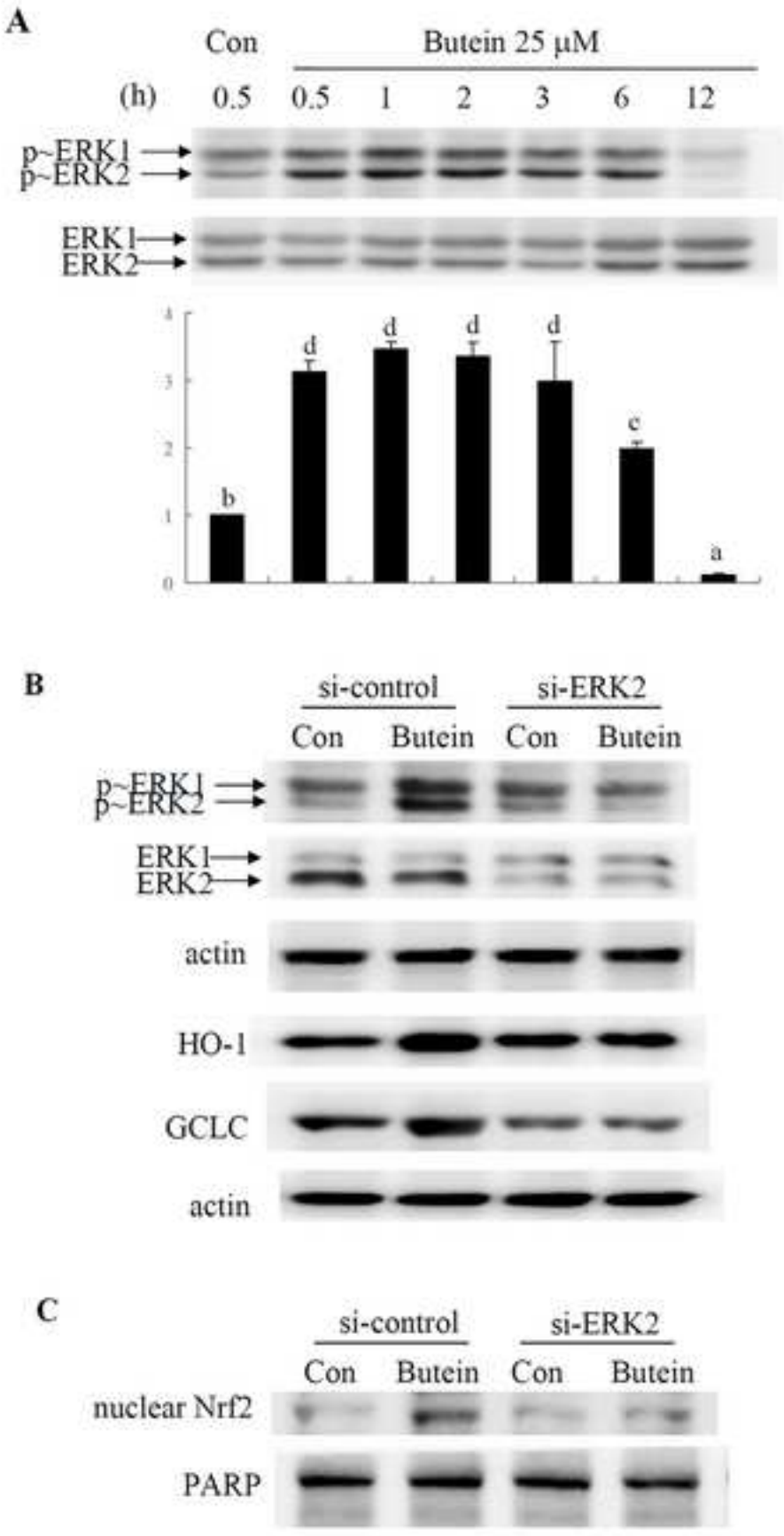

Figure(s)
Click here to download high resolution image

Fig. 5.

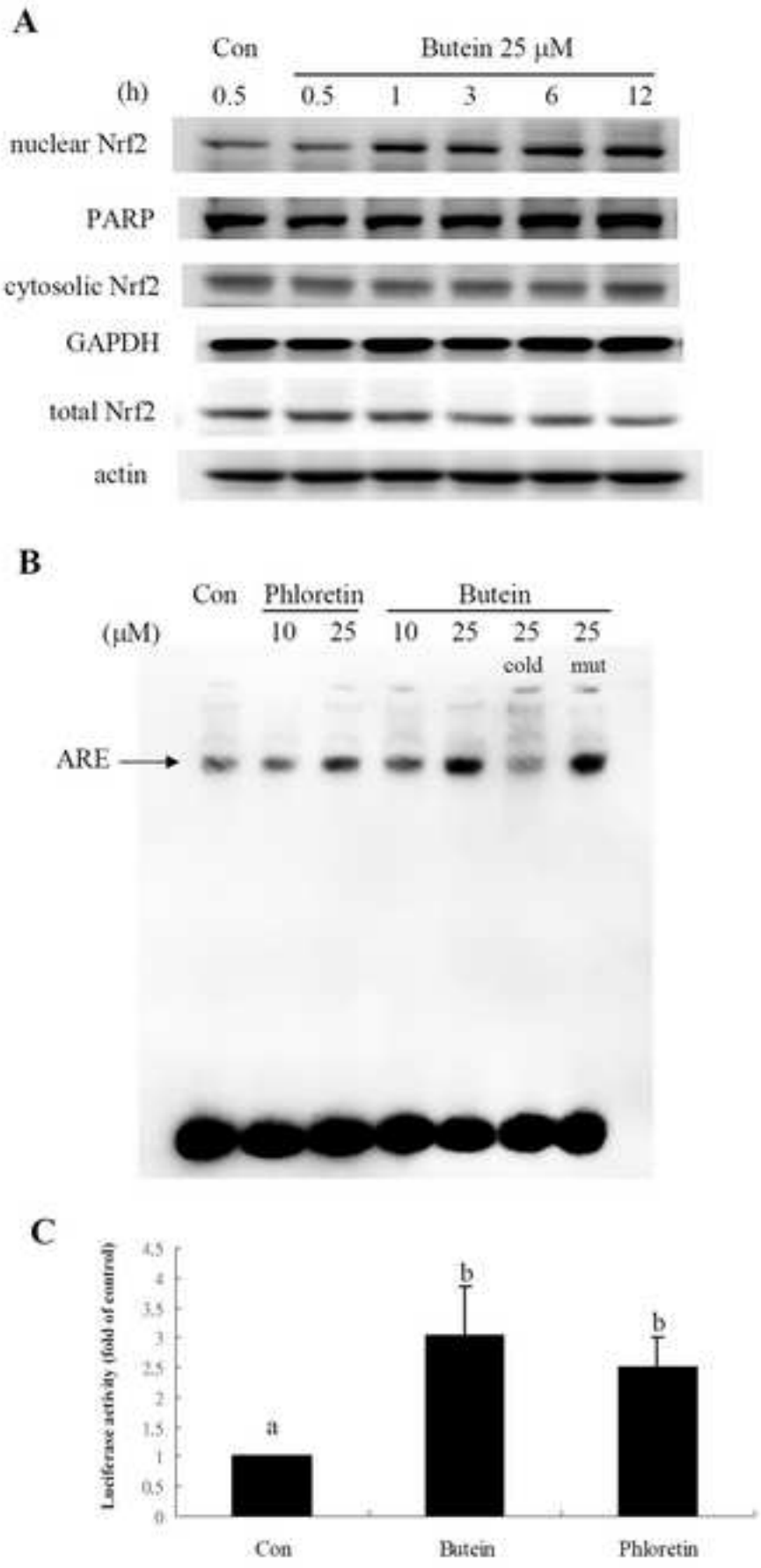

Figure(s)
Click here to download high resolution image

Fig. 6.

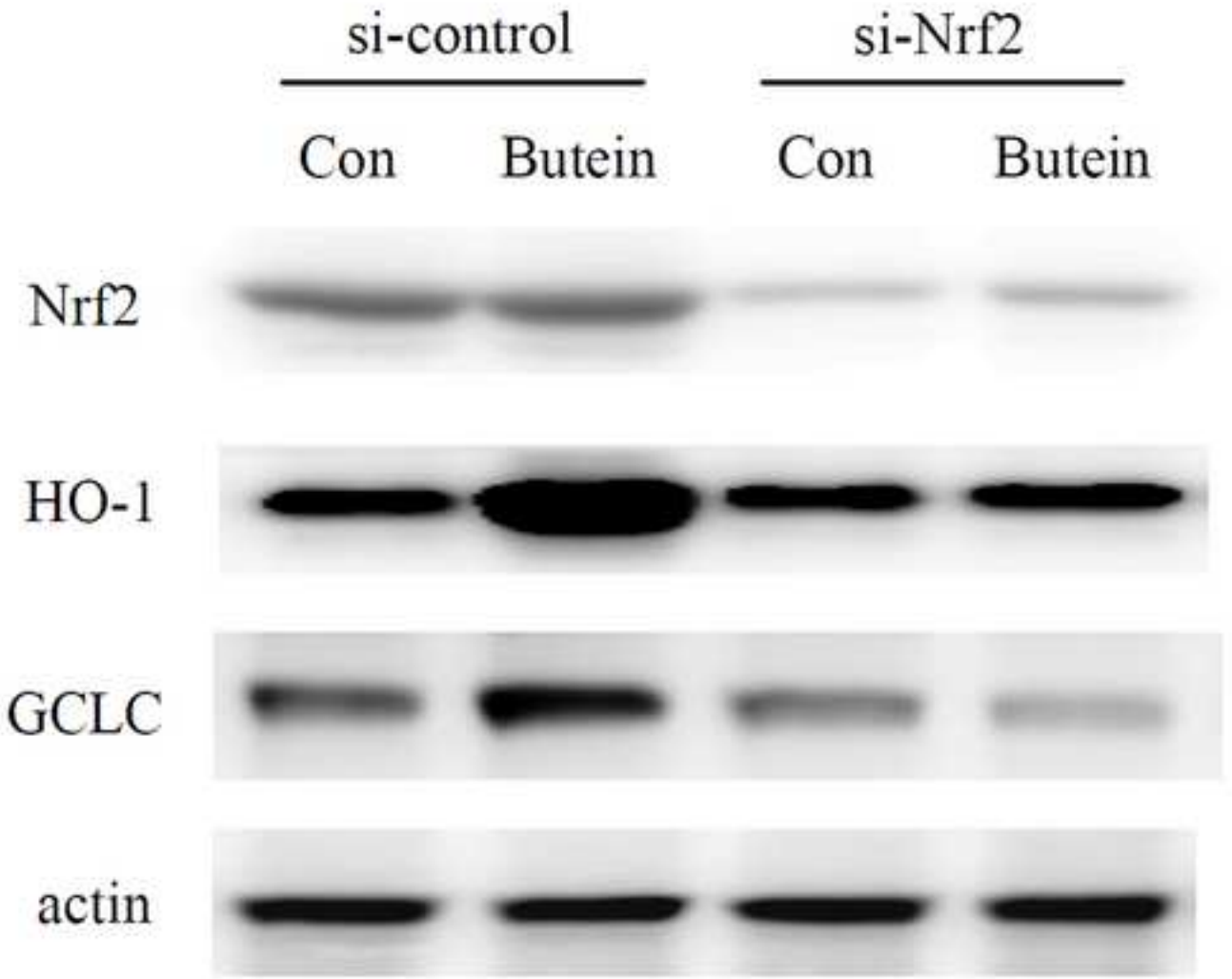

Figure(s)
Click here to download high resolution image

Fig. 7.

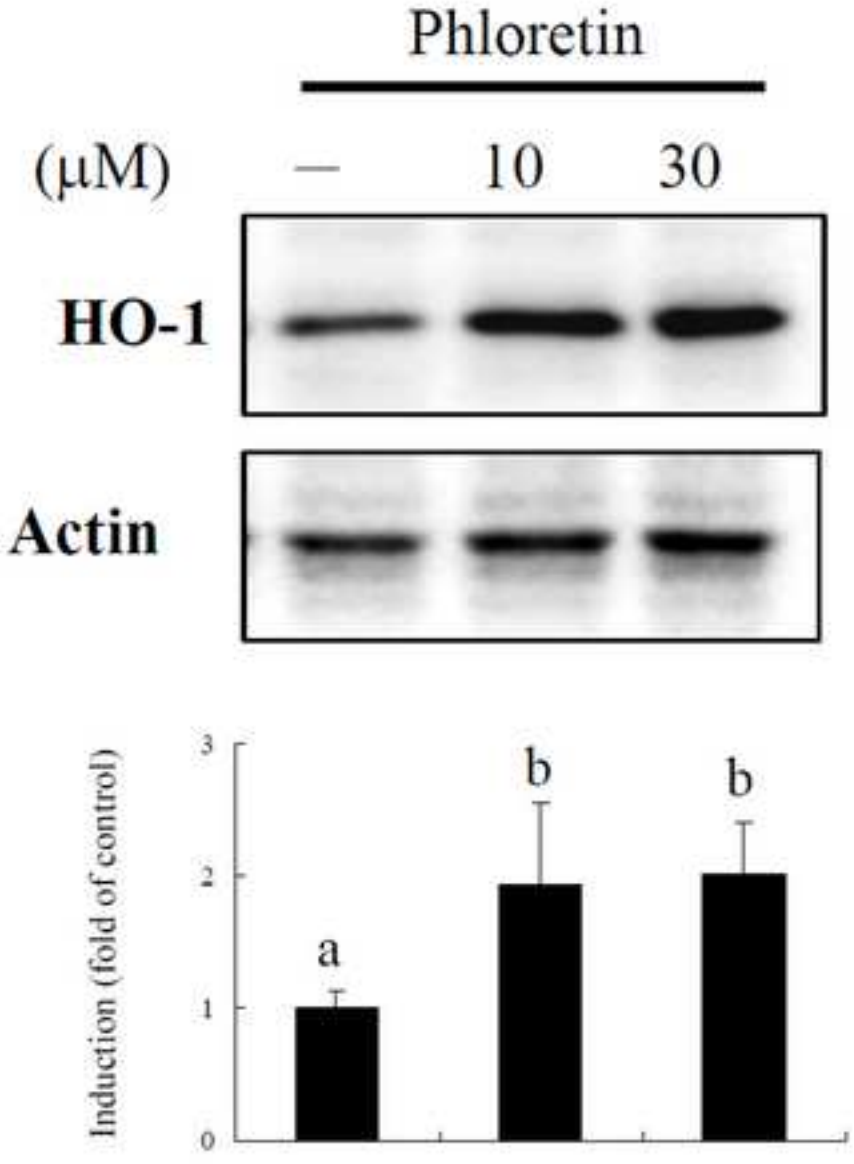

Figure(s)
Click here to download high resolution image

Fig. 8.

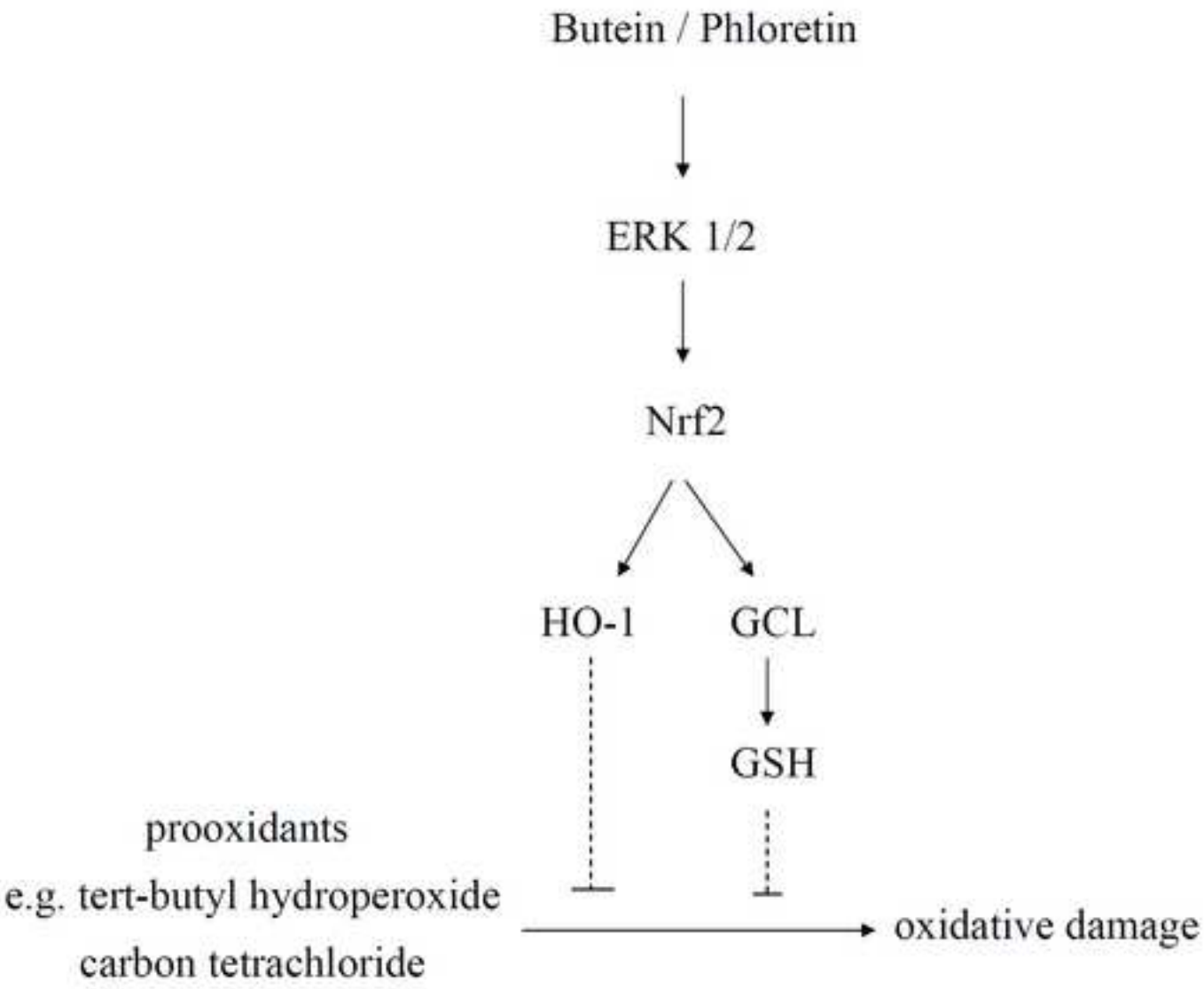

Supplementary Material

Click here to download Supplementary Material: S1-revised 1.tif